121614

NASA TN D-1537

NASA TN D-1537

29

N63 16880

TECHNICAL NOTE

D-1537

PRELIMINARY INVESTIGATION OF CATASTROPHIC FRACTURE OF LIQUID-FILLED TANKS IMPACTED BY HIGH-VELOCITY PARTICLES

By Francis S. Stepka and C. Robert Morse

Lewis Research Center
Cleveland, Ohio

NATIONAL AERONAUTICS AND SPACE ADMINISTRATION

WASHINGTON May 1963

NATIONAL AERONAUTICS AND SPACE ADMINISTRATION

TECHNICAL NOTE D-1537

PRELIMINARY INVESTIGATION OF CATASTROPHIC FRACTURE OF LIQUID-FILLED TANKS IMPACTED BY HIGH-VELOCITY PARTICLES

By Francis S. Stepka and C. Robert Morse

SUMMARY

Metal specimens acting as a wall of a liquid-filled tank were impacted by small high-speed particles. The specimens were 1/32- and 1/16-inch-thick 2014-T6 and 7075-T6 aluminum and 1/32-inch-thick 60-percent-cold-reduced AISI 301 stainless steel. The liquids used were water, glycerin, and nitrogen. The impacting particles were primarily 7/32-inch-diameter spheres of different materials and densities. Impacts were made at velocities up to 7500 feet per second.

Catastrophic fracturing, rather than simple puncturing, of tank walls made of aluminum generally resulted at impact velocities between 2850 and 6900 feet per second. No fracturing of stainless-steel specimens on water-filled tanks was obtained even at the maximum capabilities of the gun used.

The pressure pulse generated in the liquid by the impacting particle appears to be the primary cause of most of the fractures. The dynamic stresses generated in the specimen by the cratering and puncturing action of the particle and the initial static stress due to tank pressurization also contribute to the fracturing.

The characteristics of the pressure pulse generated in water-filled tanks by the impact, the velocity of propagation of the shock front generated in the water, and the time required for specimens to fracture after impact were determined. These data indicate that, for the materials and the thicknesses investigated, the pressure pulses generated in the water and the resulting forces contributing to catastrophic fracturing of the specimens are local phenomena and are independent of the tank size if the radius is greater than a few inches.

INTRODUCTION

As the vehicles grow larger and the mission times become longer, there is increasing concern over the danger of meteoroids penetrating the space vehicles (ref. 1). The hazard may be even more severe for liquid-propellant tanks because pressure forces generated in the contained liquid as a result of impact may result in catastrophic failure rather than simple penetration. Catastrophic failure is considered to exist when tearing or complete blowout of the tank wall occurs such that repairs to prevent loss of liquid while the vehicle is in flight would not be possible. This report presents the initial results of an investigation of this potential hazard.

For vehicles requiring propulsion after reaching orbital velocity, the propellant tanks will often be the components with the greatest weight and exposed area. As a result, the meteoroid problem may be of greater concern for the propellant tank than for any other component of the vehicle. The protection that may be required could have a very significant effect on total vehicle weight.

Considerable research, both experimental and analytical, has been conducted on the penetration mechanism of high-speed particles. This research, which is summarized in reference 2, was concentrated mostly on thick, unstressed targets. Some analytical studies (refs. 3 and 4) have considered the problem of punching holes in stressed sheets and have evaluated the transient stress distributions. The hole-punching process results in a stress concentration and a peak transient stress near the hole that may be approximately 10 percent higher than the static stress that would exist in a stressed sheet with the hole present. The effects of transient pressure forces within a contained liquid that result from shock waves radiating outward from the point of impact have not been considered. Under some conditions of impact, the wall stresses induced by these shock waves can reach values substantially greater than those induced by simply punching a hole in a stressed sheet.

References 5 and 6 indicate that, in the zero-gravity condition, the liquid contained in an unbaffled tank will be in contact with the tank walls and that any gas present will tend to form a pocket in the center of the tank. As a consequence, pressure rises will be generated in the contained liquid for all impacts on the tank wall regardless of the point of impact.

The importance of determining conditions that can lead to catastrophic failure of propellant tanks when impacted by small, high-velocity particles such as meteoroids is apparent from the previous discussion. Earlier investigations have not studied the combined effects of high-velocity impact on thin walls in contact with a liquid. This report, therefore, presents preliminary results from an investigation directed at obtaining an understanding of the factors affecting catastrophic propellant-tank failure resulting from high-velocity impact.

The investigation was conducted at impact velocities from 1650 to 7500 feet per second. Tank walls, 1/32 and 1/16 inch thick, made of 7075-T6 and 2014-T6 aluminum and 60-percent-cold-reduced AISI 301 stainless steel were impacted by spheres ranging from 1/16 to 7/32 inch in diameter that were made of nylon, aluminum, steel, or tungsten carbide. The contained fluids investigated were water, glycerin, and liquid nitrogen.

FACTORS AFFECTING FRACTURE

When a high-velocity particle impacts a tank wall in contact with a liquid, dynamic stresses are first induced in the wall by the cratering and puncturing action of the particle. The cratering action first induces radial compressive and circumferential tensile stresses in the wall. After the wall is penetrated, the elastic strain energy absorbed in the cratering process is released, and radial tensile and circumferential compressive stresses are induced. The puncturing action induces dynamic flexural stresses in the wall because of the resistance to shearing offered by the wall. After the particle has penetrated the wall and impacted the contained liquid, part of the kinetic energy or momentum of the particle is converted into a pressure wave that emanates from the impact point. This pressure wave induces additional stresses in the tank wall. These stresses alone, or in combination with those induced by the cratering action and the puncturing of the wall, plus any static stress in the wall due to initial tank pressurization, may be large enough to result in catastrophic fracture of the tank wall. Because the puncture has created a stress concentration region, the stress in the wall required to induce a failure is considerably less than that in a wall without a hole.

The factors affecting the stresses induced in a tank wall of a given thickness and material impacted by a high-speed particle are as follows: The dynamic stresses in the wall due to impact and penetration are functions of

(1) Particle velocity

(2) Particle material and/or density

(3) Particle size

(4) Particle shape

The stresses in the wall due to the liquid pressure are functions of

(1) Liquid static pressure

(2) Liquid density

(3) Liquid velocity of sound

(4) Liquid temperature

(5) Particle velocity

(6) Particle material and/or density

(7) Particle size

(8) Particle shape

(Some of these factors may possibly be grouped together into parameters such as particle kinetic energy or momentum and liquid compressibility.)

In addition to these factors, the catastrophic fracture of a tank wall of a given material would be affected by

(1) Amount of cold working and heat treatment

(2) Shape and size of hole and/or microcracks from impact

(3) Material strength properties at high-strain-rate loading

(4) Material strength properties at temperature of liquid

Preliminary analyses were made to relate some of the factors affecting the failure mechanism in an attempt to provide a basis for the presentation of the data and are discussed in the section RESULTS AND DISCUSSION.

APPARATUS

The test apparatus consisted of the range equipment, test tanks, test specimens, and associated instrumentation for evaluating the effect of high-velocity impact into liquid-filled containers.

Range Equipment

A .22 caliber rifle was used to accelerate the particles. The rifle was mounted on a table as shown in figure 1 and was fired remotely. The powder charges were varied to control the velocity of the particles. The impacting particles were mostly spheres of nylon, aluminum (2014-T6), steel (chrome alloy), or tungsten carbide. The sizes of the spheres ranged from 1/16 to 7/32 inch in diameter. A limited number of projectiles were copper cylinders 7/32 inch in diameter and approximately 0.6 inch long. Spherical particles smaller than the gun bore were projected by means of a sabot (fig. 1). The sabot was a nylon cylinder 0.22 inch in diameter and length.

Blast shields were located about 6 inches from the muzzle of the rifle to protect the velocity measuring sensors from damage when the rifle was discharged. A sabot deflector was located 4 inches downstream of the blast shields. This device deflected and separated the sabot from the accelerated particle. A pair of sensors to measure particle velocity was located down range from the sabot deflector. Each sensor consisted of a 0.25-mil Mylar sheet with a layer of vapor-deposited aluminum approximately 100 angstroms thick on each side of the Mylar. Penetration of each of the sensors by a particle resulted in the shorting of the two layers of aluminum of the sensor, which permitted a capacitor to discharge. The successive discharge pulses were monitored by an electronic event timer.

Test Tanks

Two types of tanks were employed in the investigation. One type was a cylindrical metal tank that was designed with one end readily removable. This removable end constituted the test specimen for each run. This type of tank was used primarily for the determination of the resistance to fracture of various materials and thicknesses as a result of impact. The other type of tank was rectangular in shape and had an open top; this tank, made of transparent plastic, had one removable end made of sheet metal that acted as the test specimen. The transparent tank was used primarily to investigate the shock waves that were propagated within the tank fluid upon impact.

Two sizes of cylindrical tanks were used. The small tank had an inside diameter of 12 inches and was 9 inches deep; the large tank was approximately 30 inches in diameter and 37 inches deep. The volumes of the two tanks were 0.6 and 15.1 cubic feet, respectively. A photograph of the two tanks and a test specimen is shown in figure 2. For the tests with water and glycerin as the contained liquid, the tanks were made of steel pipe. For the test with liquid nitrogen, an insulated aluminum alloy tank of the same size as the small steel tank was used.

The transparent plastic tanks each had a 1/32-inch-thick 7075-T6 aluminum alloy sheet as one of the walls. Two sizes of these tanks were used; one measured 1 by 1 by 1 foot and the other 2 by 2 by 1 foot. The metal sides or specimens on these tanks were 1 and 2 feet square, respectively. Only water was used in these tanks. A photograph of the large tank (after impact) is shown in figure 3.

Test Specimens

The test specimens on the metal tanks were octagonal in shape, as shown in figure 2. The test section of these specimens was a circle 11 inches in diameter. The specimens were made of two aluminum alloys, 2014-T6 and 7075-T6, and of a stainless-steel alloy, 60-percent-cold-reduced AISI 301. The aluminum specimens were 1/32 and 1/16 inch thick, and the stainless-steel specimens were 1/32 inch thick. The materials were selected because of their relatively high strength properties at cryogenic temperatures, which would probably be required for propellant-tank application.

Instrumentation

In addition to the instrumentation used to measure the velocity of the impacting particle, described in the section Range Equipment, the following instrumentation was also used. Two piezoelectric crystal pickups were located in the water of the transparent tank near the impact region to determine the local pressure change in the water with respect to time due to the pressure wave generated by the impacting particle. The pickups had an upper pressure limit of 20,000 pounds per square inch. The pickup sensing unit was approximately 3/16 inch in diameter and 5/16 inch long.

The characteristics of the pressure wave generated by impact were also evaluated visually from high-speed photographs of the progress of the shock-wave front as viewed through the side of a water-filled transparent plastic tank. A continuous writing camera with a maximum writing rate of 1.6 million frames per second was used. The damage to test specimens caused by the impact and penetration of the particles was recorded by photographing the front faces of the test specimens. In some instances a technique of photographing the front face (metal specimens) and side of the transparent water-filled tank simultaneously was employed. This photographic procedure permitted direct correlation of the specimen time to fracture with the progress of the shock wave in the liquid.

PROCEDURE

Impacts Into Specimens

The procedure was to fire the individual particles into a test specimen that was attached to a metal tank filled either with water, glycerin, or liquid nitrogen and to observe the resulting damage. Specimens were tested without an initial static stress (unstressed) and with an initial effective static stress equal to the yield strength of the material. This stress was induced by appropriate pressurization of the tank and gave a 1-to-1 biaxial stress field. The procedure used to determine the relation between static tank pressure and the initial static stress level in the specimens is described in the section Stress Level and Distribution in Specimens.

Transient Pressure Measurements

The procedures for determining the characteristics of the pressure pulse generated in water by the impact will be considered next. One of the methods used was to obtain a shadowgraph of the progress of the shock front generated by impact, as viewed through the sides of a water-filled transparent plastic tank. The progress of the shock front was obtained by observing the individual frames of photographs of the shock front taken with the high-speed framing camera. The shock-front velocity was determined from the known film framing rate and the observed motion of the shock front from frame to frame. When the shock-front velocity and the relation between this velocity in water and pressure as presented in reference 7 were known, the pressure at the shock front as it moved away from the impact point was determined. The pressure was also determined by using piezoelectric crystal pressure pickups mounted in the water-filled tanks near the impact point. The output of the gages was transmitted to an oscilloscope from which a photographic record of the traces was obtained. From the trace of the voltage output of the gage and a manufacturer's calibration of the voltage-pressure characteristics of the gage, the local pressure change of the liquid with time was determined.

RESULTS AND DISCUSSION

Several simple analytical models were considered in an attempt to relate some of the factors affecting fracture of a liquid-filled tank as a result of impact by a high-velocity particle. In all the analyses the pressure generated in the liquid by the impacting particle was considered to be the major factor influencing fracture. It was also assumed that fracture occurred before any pressure wave could be reflected from the walls of the tank. The effects of the dynamic stresses induced by the cratering action and puncturing were considered small and, therefore, were neglected; however, attempts were made to account for the loss of particle velocity when the tank wall was punctured. With these conditions imposed, analytical expressions for the pressures generated by impact were sought.

One of the models considered was one-dimensional impact of two media (ref. 2). This model provided a relation for the maximum pressure at the interface of the two media as a function of impact velocity and the acoustic impedances of the media. In an attempt to include the effect of particle size, another model was considered. For this model it was assumed that the energy absorbed by the liquid in decelerating the impacting particle is used only for pressure and change in volume of the liquid in the tank affected by impact. The drop in impact velocity through the tank wall was accounted for by using the empirical relations for residual velocity of particles after the puncture of sheet materials as presented by Malick in the "Proceedings of the Third Symposium on Hypervelocity Impact." Although some agreement with trends was indicated, applying the relations obtained to the experimental data did not provide a satisfactory correlation of the data. The simplified models and analyses used seemed to be insufficient to describe the fracture mechanism completely; therefore, a more rigorous analysis is considered necessary. For the purposes of this preliminary report, the data at conditions of fracture for each material and thickness of the tank wall and for each contained liquid will be presented; particle parameters that appear to be significant, that is, the particle kinetic energy, velocity, size, and material, will be used. Subsequent analyses may very well indicate more satisfactory parameters for presentation of the data. Presentation of these data in essentially raw form by using these parameters rather than waiting until an adequate model was developed for predicting the failures was warranted because of the current interest in the results of this preliminary investigation.

Stress Level and Distribution in Specimens

Prior to starting the primary investigation reported herein, it was necessary to determine whether a uniform stress field existed in the center or impact region of the test specimen, which was given an initial static stress by the pressurization of the liquid in the tank. It was also necessary to determine the extreme fiber stress in the test specimen in the region of impact for given values of liquid pressurization.

The extreme fiber stress in the wall was determined by measuring the curvature of the specimen associated with a given pressure within the tank and then by using the following equation, which considers the effect of both the membrane and bending stresses in the specimen:

$$S = \frac{P\left(R - \frac{t}{2}\right)}{2t} + \frac{E\left(\frac{t}{2}\right)}{R(1 - \nu)}$$

where

S extreme fiber stress, psi

P pressure in tank, lb/sq in.

R radius of curvature of outside surface of specimen, in.

t thickness of specimen, in.

E Young's modulus, psi

ν Poisson's ratio

The calculated values for the pressures required in the tank to produce extreme fiber effective stresses equal to the 0.2-percent offset yield strengths of the specimen materials, thicknesses, and temperatures investigated are listed in the following table:

Material	Liquid in tank	Temperature, °F	Yield strength, psi	Thickness, t, in.	Tank pressure required, P, lb/sq in.	Young's modulus, E, psi
7075-T6	Water	60	74,400	1/32	165	10.3×10^6
7075-T6	Nitrogen	-320	91,000	1/32	220	11.5
7075-T6	Water	60	74,400	1/16	290	10.3
2014-T6	Water	60	66,200	1/32	135	10.7
2014-T6	Water	60	66,200	1/16	214	10.7
AISI 301 (60 percent cold reduced)	Water	60	181,000	1/32	362	28

The values of Poisson's ratio ν used in the stress equation for the aluminum alloys and for the stainless steel were 0.33 and 0.30, respectively. The values of Young's modulus were obtained from unpublished data from the investigations reported in references 8 and 9. The 0.2-percent offset yield strengths of the materials presented in the table were obtained from these references. For the conditions listed in the table, the ratios of the calculated bending to membrane stress were approximately 0.15 and 0.36 for the 1/32- and 1/16-inch-thick specimens, respectively. For these conditions, the middle fibers were stressed to approximately 87 and 73 percent of the yield strengths, respectively. The bending stresses induced by the pressurization of the tank are, therefore, a significant portion of the total static stress in the specimen.

The stress distribution near the center of the specimen on a pressurized tank was determined by the use of electrical-resistance strain gages. The results indicated that, for stress levels as large as 0.8 of the 0.2-percent offset yield strength of the 2014-T6 aluminum, a uniform stress field existed within a maximum deviation of 5 percent in an area circumscribed by a $1\frac{1}{2}$-inch radius from the specimen center. The stresses as determined from the strain gages located 1/8 inch from the specimen center agreed within 5 percent with the extreme fiber stress as calculated from the stress equation.

Catastrophic Fracturing Due To Impact

A summary of the minimum particle impact velocities and kinetic energies required to fracture specimens is presented in table I. The impact capabilities of the facility were insufficient to result in catastrophic failure for some test conditions. For these cases table I also lists the maximum impact conditions investigated, although no fractures occurred. Some of the specimens were given an initial hydrostatic stress equivalent to the yield strength of the material (by pressurization of the tank) before impact by the high-velocity particle. The other specimens were not subjected to any initial stress. Each of these groups of specimens will hereinafter be designated as "stressed" and "unstressed" specimens, respectively.

Stressed aluminum specimens on water-filled tank. - Photographs of the punctures and the typical patterns of fractures that were obtained for the specimens are shown in figure 4. For the 1/32-inch-thick specimens, which had all the different patterns of fractures encountered, no relation between the number of cracks and impact energy, velocity, or particle material was observed. Examination of the fractures indicated that the plane of the fractures was generally at 45° to the specimen surface; this would indicate a shear failure. Several impacts made into partly filled tanks where the liquid level was only slightly above the impact point resulted in failures similar to those obtained on completely filled tanks.

Impacts and penetrations by particles of various sizes and different materials into specimens of one material and thickness provided data to determine the effect of particle kinetic energy, velocity, material, and size on catastrophic fracturing of the specimen. The data obtained for impacts into 1/32-inch-thick stressed 7075-T6 aluminum specimens are shown in figure 5. The data indicate that for a given 7/32-inch-diameter metal particle there is a kinetic energy and velocity below which only puncture of the specimen results and above which catastrophic failure results. It appears that a definite critical velocity or kinetic energy exists for each of the particle materials considered in the investigation, above which rupture of the specimen will occur. The data of figure 5 also indicate that for the metal particles the critical velocity increases and the critical kinetic energy decreases as the impacting particle density decreases. The critical velocities for the 7/32-inch spheres of tungsten carbide, steel, and aluminum were 2850, 3300, and 5000 feet per second, respectively, and the associated kinetic energies were 375, 260, and 215 foot-pounds, respectively.

The data of figure 5 indicate that for the 7/32-inch nylon spheres fracture of the test specimens occurred throughout the range of velocities possible with the rifle used. Examinations of the fractures of these specimens indicated that for specimens impacted at velocities of about 7000 feet per second a smooth puncture was obtained and the fracture probably resulted from the pressures generated in the water. With impacts at low particle velocities of about 1650 to 3000 feet per second, however, the specimen was bent and torn in the vicinity of the impact. This tearing action by the low-velocity nylon spheres, rather than the pressures generated in the water, was primarily responsible for the fracturing of these stressed specimens. This conclusion was verified by the fracture of specimens of 7075-T6 aluminum on the test tank filled with nitrogen gas at the same pressure as the water-filled tank and impacted by a low-velocity (about 3500 ft/sec) nylon particle. When a specimen on the pressurized gas-filled tank was impacted with a nylon sphere at about 6000 feet per second, only a puncture resulted.

In an attempt to determine the effect of particle size and material, a series of impacts was made with spheres of the following sizes and materials, in addition to the 7/32-inch sphere already mentioned: 1/8-inch steel, 1/8-inch tungsten carbide, 3/32-inch aluminum, and 1/16-inch steel. The results of impacts with these particles are also shown in figure 5. It can be seen that no catastrophic failures were achieved with any of these smaller particles even at velocities as high as 7180 feet per second. It appears, therefore, that, in addition to particle kinetic energy, velocity, and material, particle size also affects fracture. In addition, the velocity at which fracture occurs is also a function of the tank wall thickness, material, and stress level, as can be seen from the results shown in table I.

The values of critical velocities and energies as obtained from impact into 1/32-inch-thick stressed specimens of 2014-T6 aluminum alloy were approximately similar to those obtained with the 7075-T6 aluminum, except for impact with the 7/32-inch-diameter nylon spheres. Impacts by these spheres over a range of velocities from about 3100 to 7000 feet per second into the 2014-T6 alloy resulted in only a puncture compared to fracturing of the 7075-T6 alloy at velocities from 1650 to 7000 feet per second. The fracture patterns obtained with the specimens made of 2014-T6 were similar to those of the 7075-T6 aluminum.

Unstressed aluminum specimens on water-filled tank. - Impacts into unstressed 1/32-inch-thick specimens of 7075-T6 aluminum indicated that fracturing of the specimens could only be obtained with the 7/32-inch aluminum spheres at velocities above 6200 feet per second. Impacts by the nylon, steel, and tungsten carbide spheres at velocities as high as 6300, 6100, and 5000 feet per second, respectively (the maximum velocities generally obtained with the gun used), resulted in only puncturing of the specimens. Examination of the specimens in the region of penetration indicated that a permanent yielding occurred, both in the punctured and fractured specimens, because of the pressures generated in the water. The deformation on these specimens was in the form of a cusp, the base of which was about 1 inch radially from the impact point.

In order to eliminate the effect of a decrease in the velocity and kinetic energy of the particle due to the puncturing of the specimen, a group of specimens were prepunched with a 3/8-inch-diameter hole that was then sealed internally with masking tape (to contain the water). Impact was made through the masking tape into the water. These tests thus provided higher velocity impacts into the water and demonstrated the damaging effect of the generated pressures without the effects of the stresses induced in the specimen by puncturing. The results of these impacts with 7/32-inch spheres indicated that fractures of the specimens were only obtained with the metal spheres. No fractures of the specimens impacted by the nylon spheres were obtained, even at the maximum velocity of the gun. The particle velocities and kinetic energies at which fractures occurred for these specimens with the prepunched hole were less than those required to fracture the specimens without prepunched holes (table I).

Stainless-steel specimens on water-filled tank. - Fracture of the 1/32-inch-thick stressed and unstressed 60-percent-cold-reduced AISI 301 stainless-steel specimens could not be obtained with the 7/32-inch-diameter spheres, even at the maximum velocities attainable with the rifle. Also, no fractures resulted when a heavier particle (a 7/32-in.-diam. by 0.6-in.-long cylinder of copper) impacted the specimen at velocities as high as 4900 feet per second. The associated kinetic energy of impact was 2365 foot-pounds. The weight of this impacting particle was about twice that of the heaviest sphere used. No further investigation of the stainless-steel specimens was undertaken with the present gun facility. As part of the investigation reported by Lovelace in the "Proceedings of the Fourth Symposium on Hypervelocity Impact," several impacts into water-filled stainless-steel tanks resulted in catastrophic fractures of the tanks. These fractures, however, were obtained at velocities and kinetic energies that were higher than in the present investigation.

Specimens on glycerin-filled tank. - In order to investigate the effect of liquid compressibility on the fracture mechanism, glycerin, which is approximately half as compressible as water, was used as the liquid in the tank. Because of its lower compressibility, it was expected to develop a stronger shock wave. For these tests, impacts were made only into unstressed 1/32-inch-thick 7075-T6 aluminum specimens. The results are shown in table I, and, as would be expected, indicate that lower impact velocities fractured the specimens on the glycerin-filled tank than on the water-filled tank. The velocities, however, were not much different. The velocity required to fracture the specimens on the glycerin-filled tank was 5900 feet per second for both aluminum and steel spheres. Fractures of specimens on the water-filled tank were obtained at 6200 feet per second with the aluminum spheres but could not be obtained with the steel spheres, even at velocities up to 6100 feet per second. Examination of the specimens after the impacts indicated that the fracture patterns were similar to those obtained on the water-filled tank, but that the deformation of the specimens was somewhat greater than those obtained on the water-filled tank. These results gave qualitative if not quantitative verification to the effect of liquid compressibility.

Specimens on liquid-nitrogen-filled tank. - The propellants currently being considered for space vehicles include cryogenic liquids. Because of the low operating temperatures of materials in contact with these liquids, the properties of the materials, such as ultimate strength, ductility, and notch strength, are frequently different from room-temperature properties. To investigate the effects of a cryogenic liquid, impacts were made into specimens on a test tank containing liquid nitrogen (boiling point of -320° F at standard atmospheric pressure). Nitrogen was used because of its ease and safety of handling as compared to other cryogenic propellants, such as oxygen and hydrogen. The nitrogen, nevertheless, provides a low temperature that is only slightly lower than that of liquid oxygen. The compressibility of liquid nitrogen is less than that of liquid hydrogen but greater than that of liquid oxygen.

Typical fractures of the stressed and unstressed 1/32-inch-thick 7075-T6 aluminum specimens on a liquid-nitrogen-filled tank as obtained from impact by 7/32-inch-diameter spheres are shown in figure 6. Comparison with figure 4 shows that a much more severe fracturing of the specimens was evident when the contained fluid was liquid nitrogen. Examination of the fractures indicated a brittle-type fracture as evidenced by the fracture being perpendicular to the specimen wall.

The critical velocities or kinetic energies for specimens on the liquid-nitrogen-filled tank were only determined for the 1/32-inch-thick 7075-T6 aluminum alloy impacted by the 7/32-inch aluminum spheres only. The results obtained indicate that the critical velocities of 5100 and 6900 feet per second for the stressed and unstressed tanks, respectively, are slightly higher than those obtained for specimens on the water-filled tank. This is what might be expected because the greater compressibility of nitrogen as compared to that of water would require higher velocities of impact to generate the pressure to cause fracture. An increase in the yield strength and notch sensitivity of the specimens, the effect of the low temperature, is present also. Based on these results with liquid nitrogen and those with water and glycerin, which demonstrated the small effect of liquid compressibility, it would be expected that the velocities required to fracture specimens on a liquid-oxygen-filled tank would be approximately the same as for a liquid-nitrogen-filled tank.

Pressure Change Characteristics of Liquid Due To Particle Impact

In order to obtain an understanding of the characteristics of the pressure pulse generated in a liquid by impact of a high-velocity particle and its contribution to fracture, measurements were made of the pressures generated. Only water was used as the liquid.

This phase of the investigation was conducted by using the transparent plastic tanks. Because of the limited number of impacts that were to be made for this phase of the investigation, maximum velocities of impact into the water were desired. In order to accomplish this, impact was made into the water through a prepunched hole in the 1/32-inch-thick sheet of 7075-T6 aluminum that formed the front face of the plastic test tank. The punched hole was sealed internally with masking tape to contain the water. Typical photographs of the progress of the shock front in the water at various times after impact are shown in figure 7. The pressure wave was generated by an impact of a 7/32-inch aluminum sphere with a velocity of 6690 feet per second. It can be seen that the shock front is hemispherical for all times and that the center remains fixed at the point of impact. A plot of the shock-front velocity and pressure in the water as functions of distance from the impact point for the impact conditions just described is shown in figure 8. The pressure was determined from the shock-front velocity as described in the section PROCEDURE. The data indicate that pressures of about 70,000 pounds per square inch are generated within 0.6 inch of the impact region and that the pressure decays rapidly with distance and approaches ambient pressure about 5 inches from the impact point. For impacts at higher velocities, pressures in excess of 100,000 pounds per square inch were indicated.

Measurements of the pressure of the passing shock wave made by piezoelectric crystal pickups located at distances of 1.44 and 1.87 inches from the impact point for the impact conditions just discussed are shown in figure 9. The dashed curves are the voltage output from the crystal pickups converted into pressure of the passing wave. The oscillations are due to the response and natural frequency characteristics of the pickups. The pressures of the passing wave are the mean of the fluctuating values. Smooth curves through the mean values are shown in the figure. Because of the response characteristics of the pickups, the mean values of pressures are valid only after 6 microseconds from the time the pressure wave is first detected by the pickups. No extrapolation of the pressure curve was attempted to predict the pressure of the passing wave front at zero time. Therefore, no comparison with the pressures at the shock front as determined from the measured shock-front velocity, as previously described, could be made. The measurements indicate a rapid decay of pressure with time. In addition, the pickups did not disclose any additional pulses of significance after the passage of the shock wave front.

Effect of Tank Size

Based on the results presented in the previous section, it would be expected that the initiation of the fracture would occur within the time duration of the pressure pulse. Also, if edge effects are not to influence the failure, fracture should occur before the longitudinal wave in the wall of the specimen travels from the impact point to the edge of the specimen and back. For the aluminum specimens in the metal tanks, which had a clamping ring with an inside diameter of 11 inches, this time would be 41.8 microseconds, based on a longitudinal propagation velocity of 20,900 feet per second for aluminum. To verify these assumptions, high-speed photographs were taken of the impact into the water through the prepunched hole in the test specimen and of the resulting fracture of the specimen. A sequence of photographs of the event is shown in figure 10. Examination of the series of photographs indicates a possible crack 13.5 microseconds after impact and a definite crack 27 microseconds after impact. Photographs for later times show the progress of fracturing and the eruption of water from the tank. The impact was made by a 7/32-inch aluminum sphere at a velocity of about 6200 feet per second. Even if fracture of the specimen had occurred as late as 27 microseconds (observation of cracks at earlier times is somewhat obscured by the water spray), the aforementioned assumptions are verified. Based on the progress of the shock front generated by the impact, the front would have advanced only about 2 inches away from the impact point in the time required for the specimen to fracture. This would indicate that only the volume of the tank contained within the hemispherical wave front of about a few inches is affected by the impact before fracturing of the specimen has occurred, and that the pressure rise and the resulting damaging forces that cause fracturing of the specimen, being local phenomena, are independent of tank size larger than a few inches.

To determine whether time to fracture is significantly different for the different thicknesses of specimens, impacts were made into 1/32- and 1/16-inch-thick stressed specimens of 7075-T6 aluminum while high-speed photographs were taken of the process. Impacts by 7/32-inch aluminum spheres resulted in fractures in 27 and 33 microseconds or less for the 1/32- and 1/16-inch-thick specimens, respectively. A sequence of photographs of the impact and the resulting fracture of the 1/32-inch stressed specimen is shown in figure 11. For an impact into a stressed 1/32-inch-thick specimen of 7075-T6 aluminum on a liquid-nitrogen-filled tank, fracture was observed 40 microseconds after impact. The time could have been considerably less, but a frost layer made detection of a crack difficult.

As further verification that impact conditions affecting fracture are essentially independent of tank size, impacts were made into specimens attached to a tank 25 times larger in volume than the 0.6-cubic-foot tank used for the results just discussed. Water was used as the liquid. The results obtained, shown in table I, indicate no significant effect of tank size. The velocities reported in table I for the impact of nylon spheres into stressed specimens of 7075-T6 aluminum on the two sizes of tanks are not the critical or minimum values at which fracture would occur, but were the lowest velocities at which impacts were made and fractures obtained. The tests were not continued with these particles at lower velocities because the fractures obtained were caused by the bending and tearing action of these particles rather than by the pressures generated in the liquid, with which this report is particularly concerned.

Space Hazard

The effects of meteoroid impacts cannot quantitatively be predicted from the results of this preliminary investigation because of the relatively low velocities of impact as compared to those expected of meteoroids. The results, however, indicate that a possible hazard to liquid-filled containers or components of vehicles in a space environment may exist if they are impacted by particles of sufficient energies and velocities. The energies required for catastrophic failure are generally in excess of those required for simple penetrations. As a result, if the vehicle has been designed with a low probability of being penetrated, the probability of catastrophic failure from meteoroid impact would be quite small.

SUMMARY OF RESULTS

The following are the results of a preliminary experimental investigation of the effects of impact by small high-velocity particles into sheet-metal test specimens attached to and acting as walls of liquid-filled tanks:

1. Catastrophic fracturing of specimens rather than simple puncturing was obtained on liquid-filled tanks when the impact velocity exceeded a critical value, which is dependent on particle size, particle density and/or material, specimen material and thickness, initial static stress level in the specimen before impact, and liquid contained in the tank.

2. Impacts into partly filled tanks, where the liquid level was only slightly above the impact point, resulted in failures similar to those obtained on completely filled tanks.

3. Catastrophic fracturing of gas-pressurized tanks also resulted from impacts by low-velocity deformable projectiles (nylon spheres), because of bending and tearing, rather than the smooth puncturing of the tank walls. High-velocity impacts by these projectiles into gas-pressurized tanks, on the other hand, resulted in smoothly-punctured holes and no fracturing of the walls.

4. Tank walls of AISI 301 stainless steel initially stressed to the yield stress by the contained water were more resistant to fracture from the additional stresses induced by the impacting particle than walls of 2014-T6 and 7075-T6 aluminum of the same thickness. No fractures of the walls made of the stainless steel were obtained within the capabilities of the gun used.

5. Effects of compressibility of the contained liquid on fracturing of specimens were obtained and found to be small. Only slightly higher impact velocities were required to fracture specimens on tanks containing glycerin (about one-half as compressible as water) than to fracture specimens on water-filled tanks.

6. The combined effects of lower liquid temperature and greater compressibility on the impact velocity required to fracture the 7075-T6 aluminum specimens were also found to be small. This was determined from impacts into liquid-nitrogen-filled tanks. The resulting fractures, however, were more severe than those obtained on water-filled tanks.

7. The pressure pulses generated in the water-filled tanks by the impacting particles were large but decayed rapidly and approached ambient pressures within about 5 inches from the point of impact. Pressures in excess of 100,000 pounds per square inch were generated as close to the impact point as 0.6 inch.

8. The shock front generated in the water-filled tank traveled only a few inches from the point of impact before fracture of the tank wall occurred. Fractures of the tank wall occurred between 27 and 40 microseconds after impact. For the thicknesses of materials investigated, the pressure pulse generated in water and the resulting forces contributing to the initial fracture of the tank walls were local phenomena and were independent of tank size greater than a few inch radius. As further verification, impacts were made into two sizes of water-filled tanks whose volumes differed by a ratio of 25; there was no significant effect of tank size.

9. This investigation indicated that, although particles of sufficient velocity and energy can result in catastrophic failure of liquid-filled tanks, the energy required for such failures is generally considerably in excess of that required for simple penetration. As a result, the probability of catastrophic failure from meteoroid impact is quite small if the vehicle has been designed with a low probability of being penetrated by meteoroids.

Lewis Research Center
National Aeronautics and Space Administration
Cleveland, Ohio, January 26, 1963

REFERENCES

1. Davison, Elmer, H., and Winslow, Paul C., Jr.: Space Debris Hazard Evaluation. NASA TN D-1105, 1961.

2. Herrmann, Walter, and Jonas, Arfon H.: Survey of Hypervelocity Impact Information. Tech. Rep. 99-1, M.I.T., Oct. 1961.

3. Miklowitz, Julius: The Dynamic Stresses Emanating from a Suddenly Punched Hole in an Initially Stretched Elastic Plate. GM-TR-259, Ramo-Wooldridge Corp., Oct. 10, 1957.

4. Miklowitz, Julius: Tensile Circumferential Stresses Created by the Unloading Mechanism of a Suddenly Punched Hole in a Stretched Elastic Plate. GM-TR-0165-00380, Space Tech. Lab., Apr. 24, 1958.

5. Reynolds, William, C.: Hydrodynamic Considerations for the Design of Systems for Very Low Gravity Environments. Rep. LG-1, Stanford Univ., Sept. 1, 1961.

6. Petrash, Donald A., Zappa, Robert F., and Otto, Edward W.: Experimental Study of the Effects of Weightlessness on the Configuration of Mercury and Alchohol in Spherical Tanks. NASA TN D-1197, 1962.

7. Cole, Robert H.: Underwater Explosions. Princeton Univ. Press, 1948, pp. 36-47.

8. Hanson, M. P., Stickley, G. W., and Richards, H. T.: Sharp-Notch Behavior of Some High-Strength Sheet Aluminum Alloys and Welded Joints at 75°, -320°, and -423° F. Spec. Tech. Pub. 287, Symposium on Low-Temperature Properties of High-Strength Aircraft and Missile Materials, ASTM, 1960.

9. Hanson, Morgan P.: Smooth and Sharp-Notch Tensile Properties of Cold-Reduced AISI 301 and 304L Stainless-Steel Sheet at 75°, -320°, and -423° F. NASA TN D-592, 1961.

TABLE I. - SUMMARY OF MAXIMUM IMPACT CONDITIONS AND MINIMUM CONDITIONS FOR FRACTURING OF LIQUID-FILLED TANKS

Specimen			Tank		Particle							
Material	Thickness, t, in.	Ratio of initial static stress to yield strength	Liquid	Volume, cu ft	Diameter, in.	Material	Density, lb/cu in.	Weight, lb	Minimum conditions for fracture		Maximum impact conditions (no fractures obtainable)	
									Velocity, ft/sec	Kinetic energy, ft-lb	Velocity, ft/sec	Kinetic energy, ft-lb
7075-T6 aluminum	1/32	1.0	Water	0.6	7/32	Nylon	0.042	2.31×10^{-4}	[a]1650	[a]9.8	----	-----
						Aluminum	.101	5.53	5000	215	----	-----
						Steel	.281	15.41	3300	260	----	-----
						Tungsten	.540	29.64	2850	375	----	-----
					1/8	Steel	0.281	2.87×10^{-4}	----	-----	7180	230
					1/8	Tungsten	.540	5.50	----	-----	7120	432
					3/32	Aluminum	.101	.428	----	-----	6580	28.7
					1/16	Steel	.281	.357	----	-----	7050	27.5
	1/16	1.0	Water	0.6	7/32	Nylon	0.042	2.31×10^{-4}	----	-----	6800	165
						Aluminum	.101	5.53	5700	280	----	-----
						Steel	.281	15.41	----	-----	6000	860
						Tungsten	.540	29.64	3000	414	----	-----
	1/32	0	Water	0.6	7/32	Nylon	0.042	2.31×10^{-4}	----	-----	6300	140
						Aluminum	.101	5.53	6200	330	----	-----
						Steel	.281	15.41	----	-----	6100	890
						Tungsten	.540	29.64	----	-----	5000	1150
		[b]0	Water	0.6	7/32	Nylon	0.042	2.31×10^{-4}	----	-----	6300	140
						Aluminum	.101	5.53	4950	210	----	-----
						Steel	.281	15.41	4900	575	----	-----
						Tungsten	.540	29.64	3700	630	----	-----
		0	Glycerin	0.6	7/32	Nylon	0.042	2.31×10^{-4}	----	-----	6900	170
						Aluminum	.101	5.53	5900	300	----	-----
						Steel	.281	15.41	5900	830	----	-----
		1.0	Nitrogen	0.6	7/32	Aluminum	0.101	5.53×10^{-4}	5100	223	----	-----
		0	Nitrogen	0.6	7/32	Aluminum	.101	5.53	6900	385	----	-----
		1.0	Water	15.1	7/32	Nylon	0.042	2.31×10^{-4}	[a]4000	[a]57	----	-----
						Aluminum	.101	5.53	5500	259	----	-----
						Steel	.281	15.41	3700	325	----	-----
2014-T6 aluminum	1/32	1.0	Water	0.6	7/32	Nylon	0.042	2.31×10^{-4}	----	-----	7000	175
						Aluminum	.101	5.53	4700	190	----	-----
						Steel	.281	15.41	4800	550	----	-----
						Tungsten	.540	29.64	2900	385	----	-----
	1/16	1.0	Water	0.6	7/32	Nylon	0.042	2.31×10^{-4}	----	-----	6500	152
						Aluminum	.101	5.53	5700	280	----	-----
						Steel	.281	15.41	5800	805	----	-----
						Tungsten	.540	29.64	4300	850	----	-----
	1/32	1.0	Water	15.1	7/32	Nylon	0.042	2.31×10^{-4}	----	-----	6000	130
						Aluminum	.101	5.53	4800	198	----	-----
						Steel	.281	15.41	3600	310	----	-----
AISI 301 stainless steel	1/32	0	Water	0.6	7/32	Aluminum	0.101	5.53×10^{-4}	----	-----	6500	363
						Tungsten	.540	29.64	----	-----	5000	1150
						Copper (cylinder)	.321	63.43	----	-----	4900	2365
		1.0	Water	0.6	7/32	Copper (cylinder)	0.321	63.43×10^{-4}	----	-----	3900	1500
						Nylon	.042	2.31	----	-----	6800	165
						Steel	.281	15.41	----	-----	5000	600

[a]Not minimum; test terminated at this condition.

[b]Wall prepunched and hole covered with masking tape.

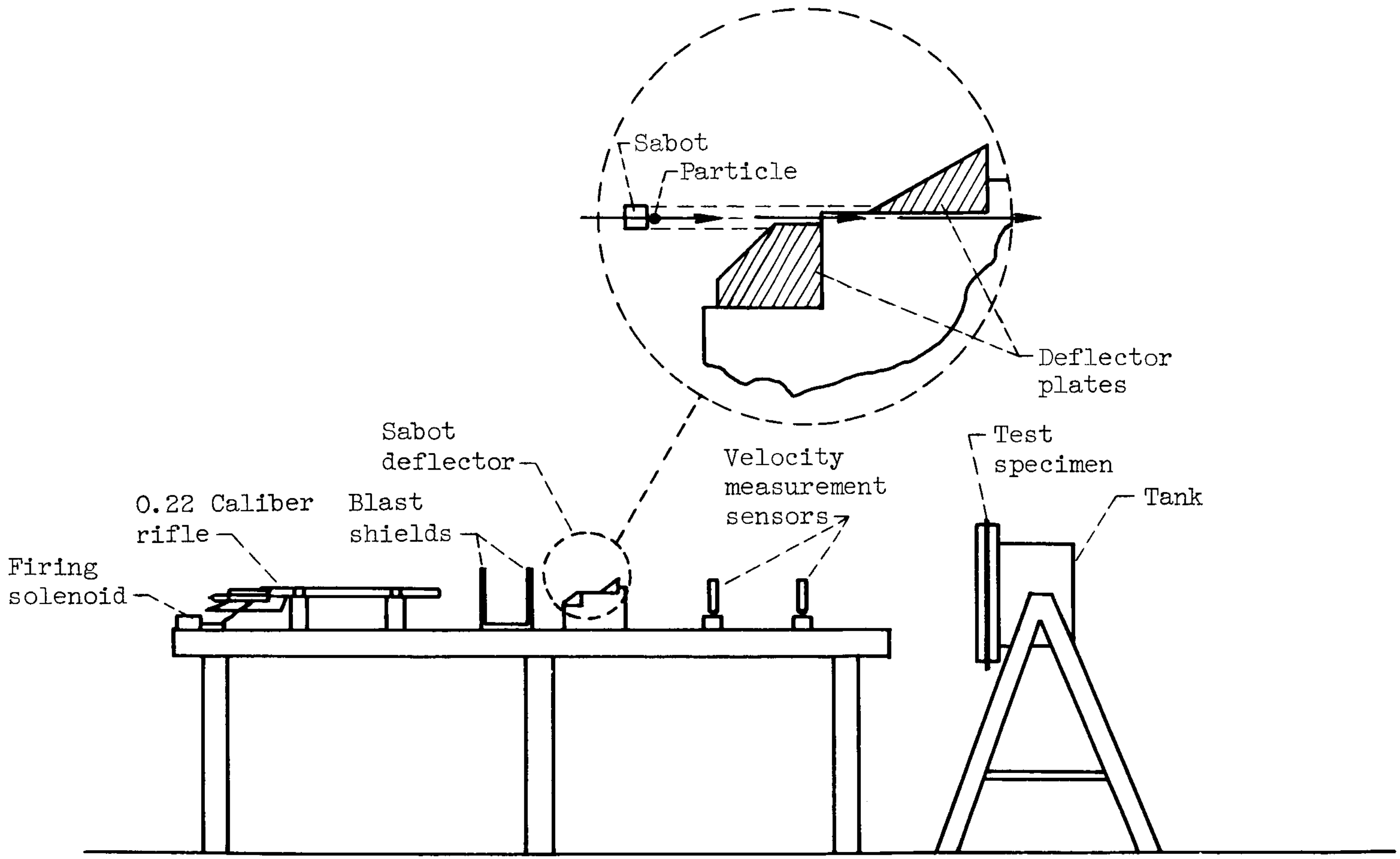

Figure 1. - Apparatus for investigation of fracture by high-velocity particles.

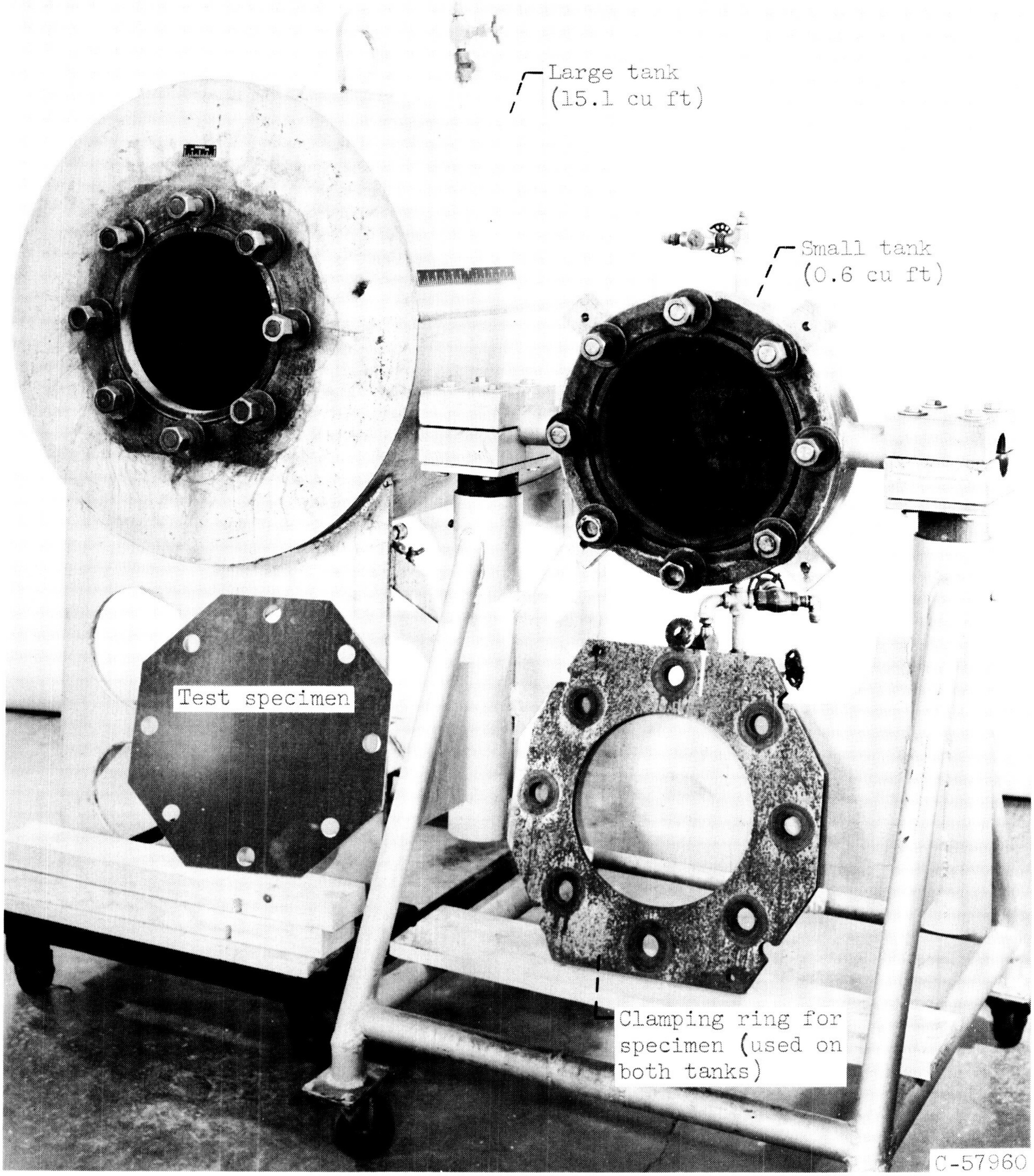

Figure 2. - Cylindrical steel tanks used in investigation of fracture by high-velocity particles.

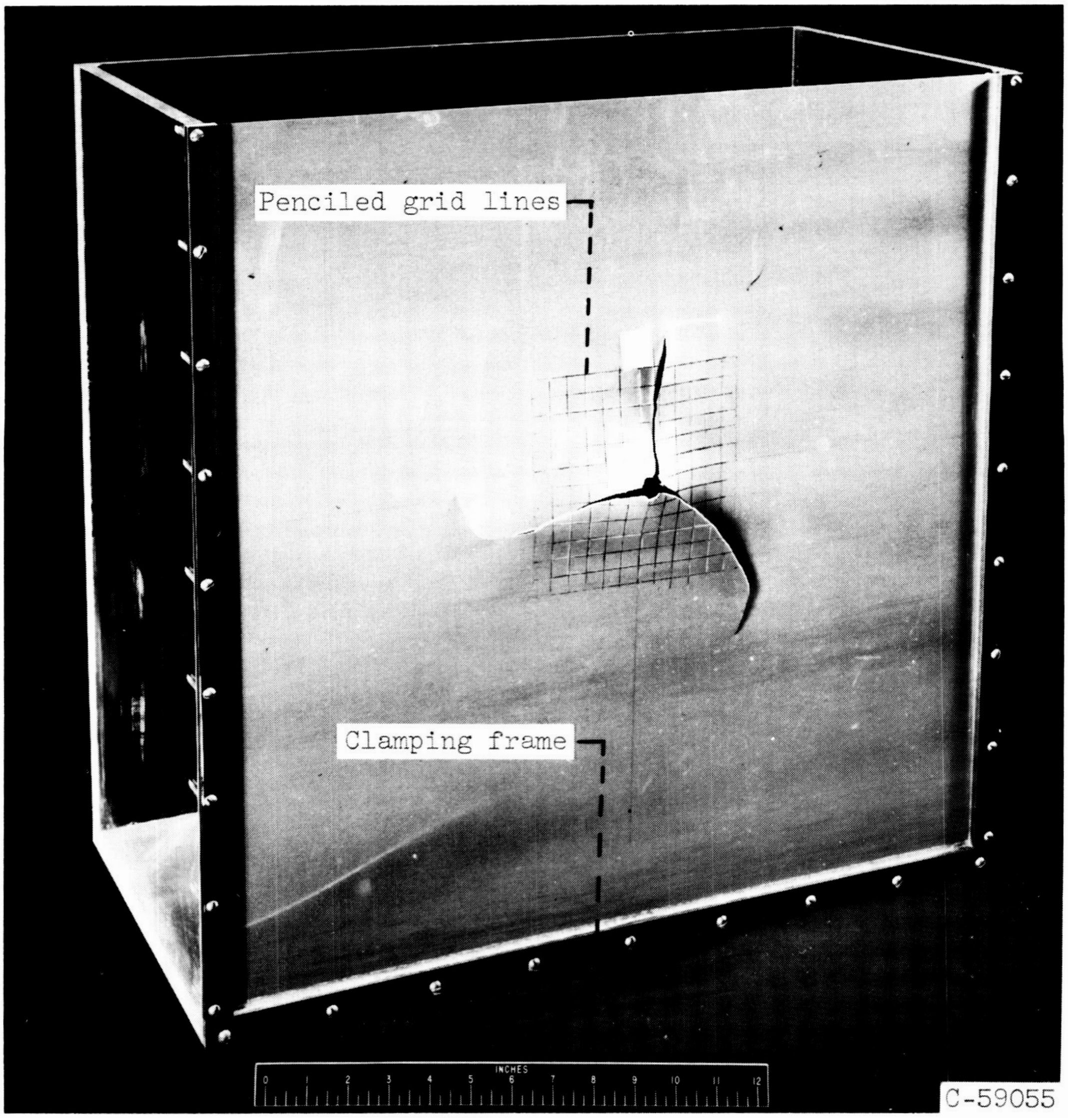

Figure 3. - Transparent plastic tank with impacted front face of 1/32-inch-thick 7075-T6 aluminum.

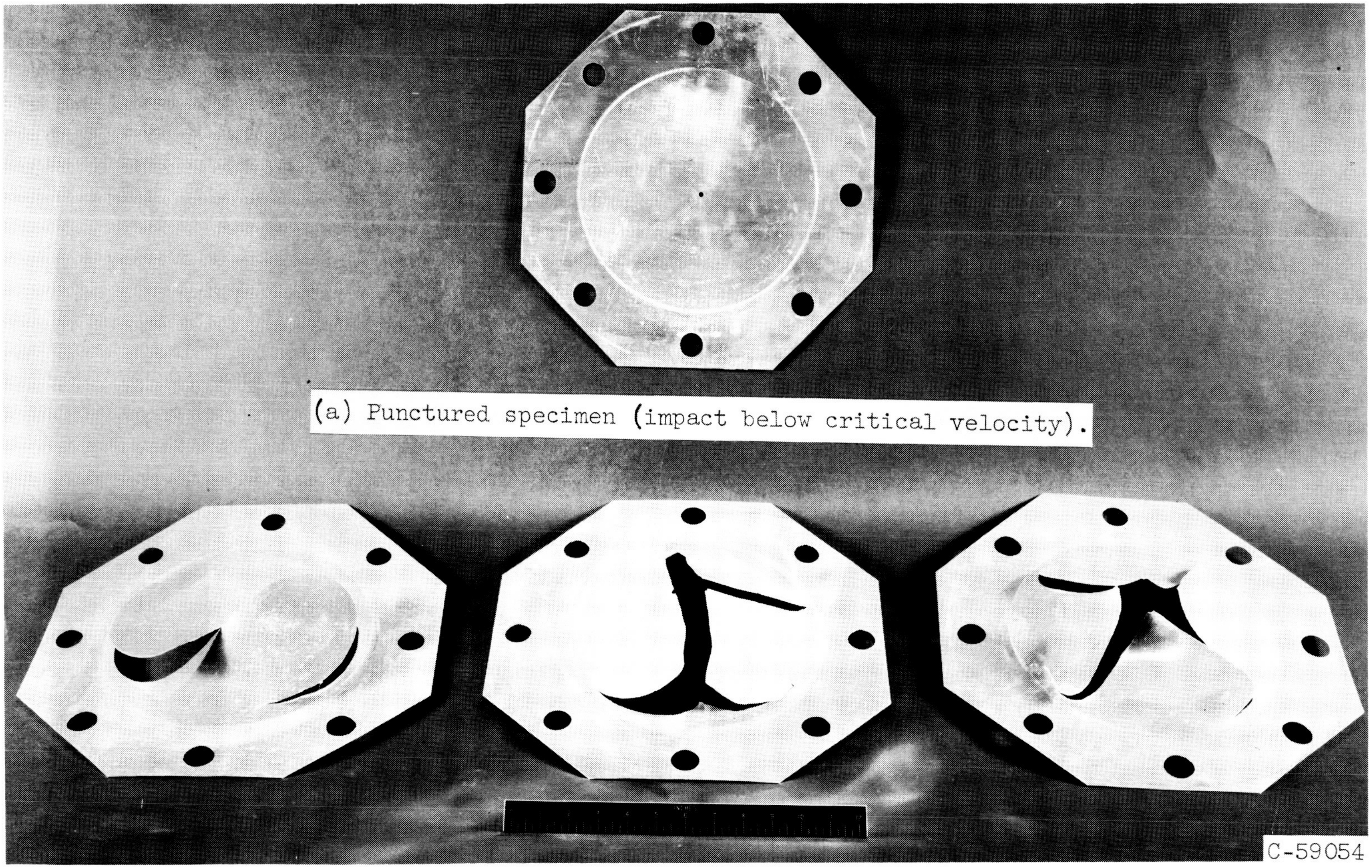

(a) Punctured specimen (impact below critical velocity).

(b) Fractured specimens (impacts above critical velocity).

Figure 4. - Results of impact by 7/32-inch spheres into stressed specimens of 7075-T6 aluminum on water-filled tank.

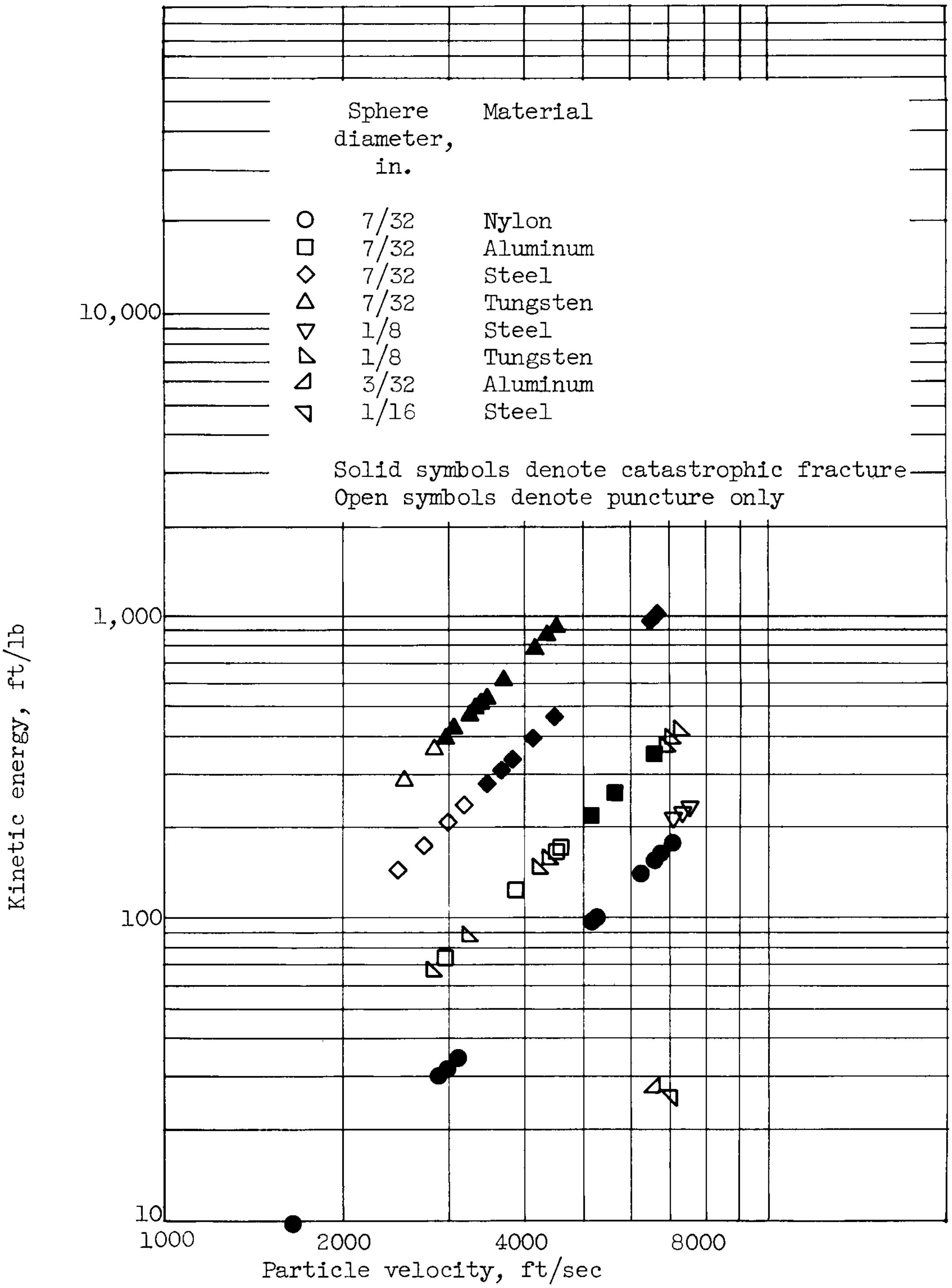

Figure 5. - Particle kinetic energy and velocity for impacts into 1/32-inch-thick 7075-T6 aluminum specimens on a water-filled tank pressurized to stress specimen to yield strength.

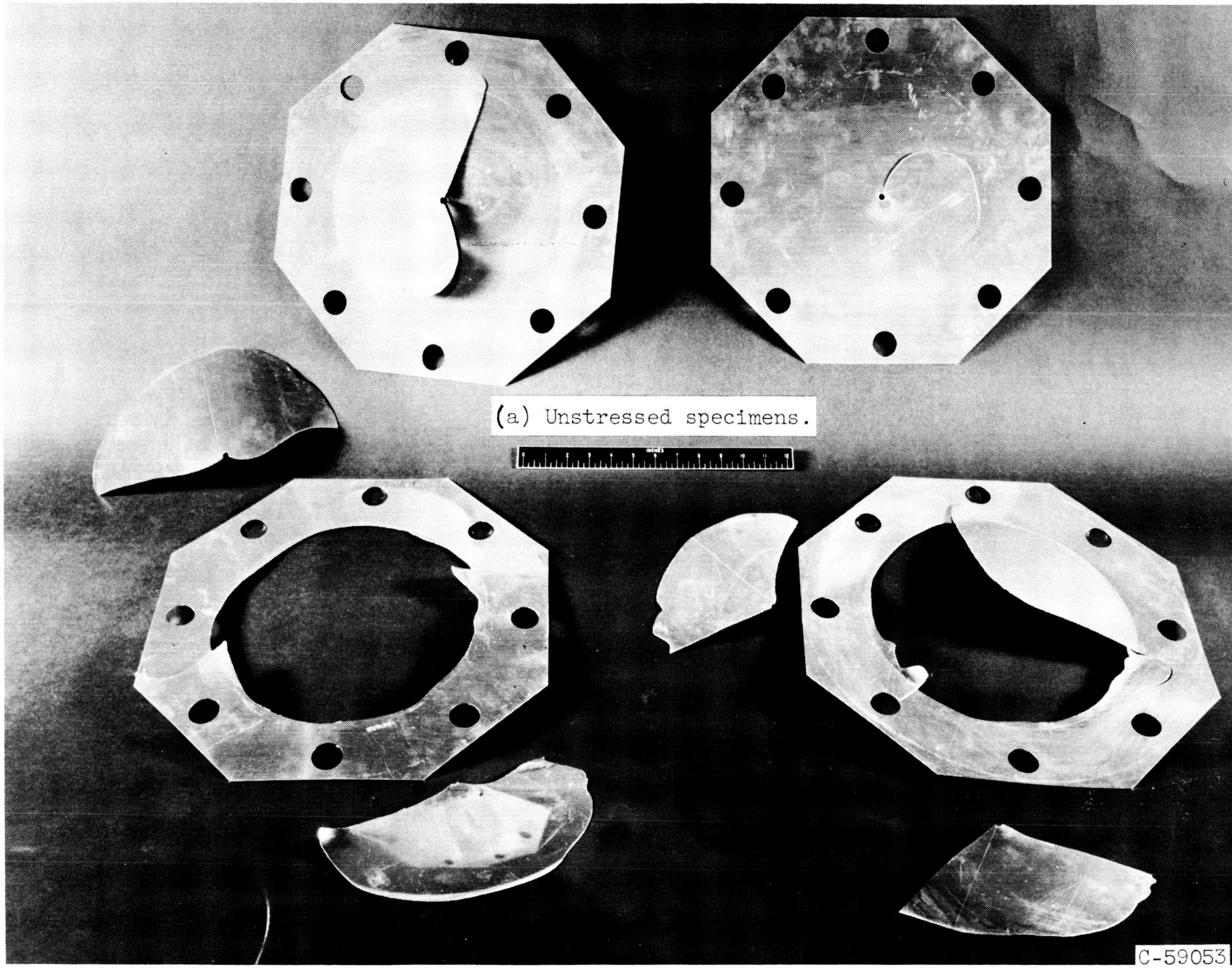

(b) Stressed specimens.

Figure 6. - Results of impacts by 7/32-inch spheres above critical velocities into 1/32-inch-thick specimens of 7075-T6 aluminum on liquid-nitrogen-filled tank.

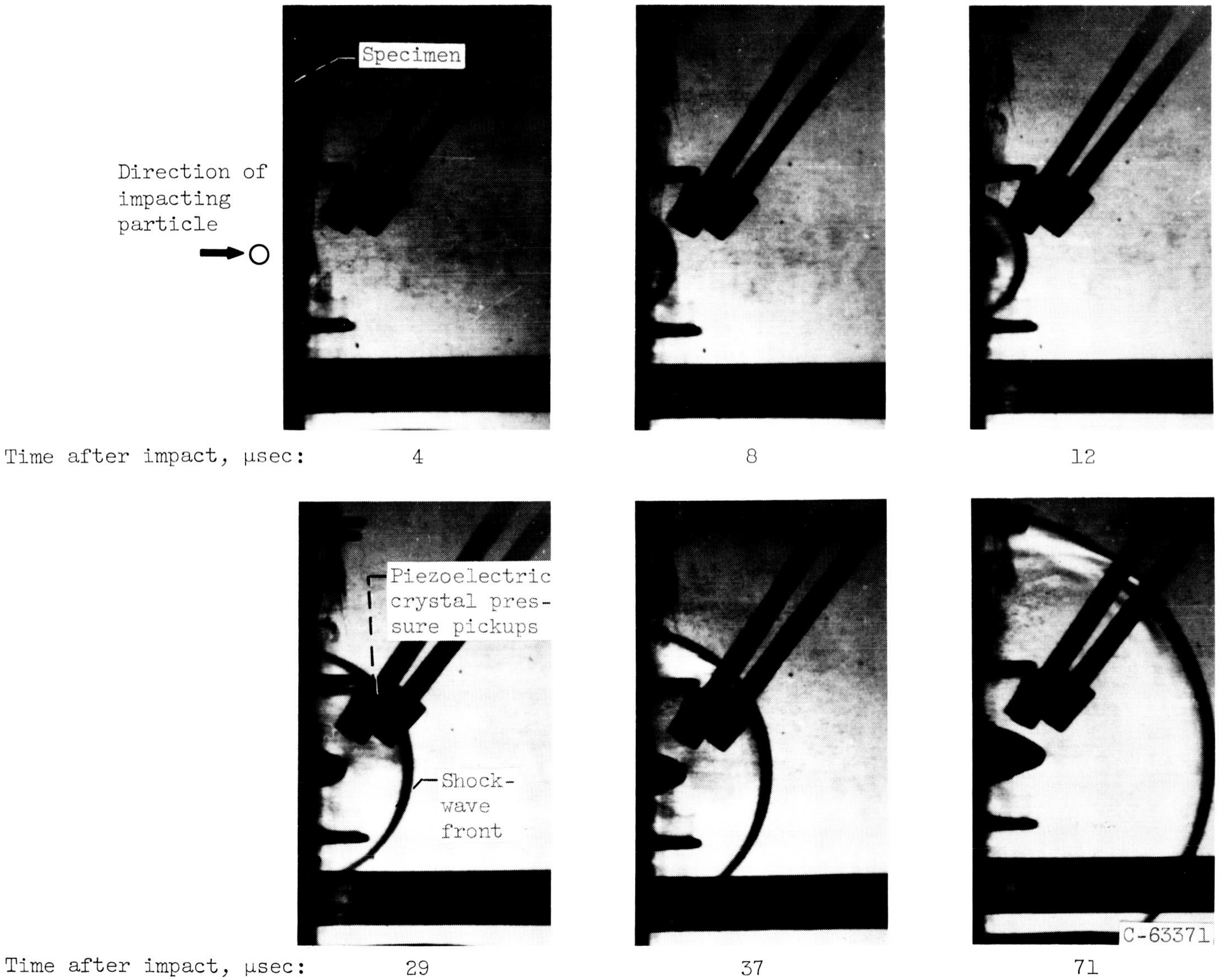

Figure 7. - Propagation of shock produced by high-velocity particle impacting water-filled transparent plastic tank. Impacting particle, 7/32-inch aluminum sphere; velocity, approximately 6690 feet per second.

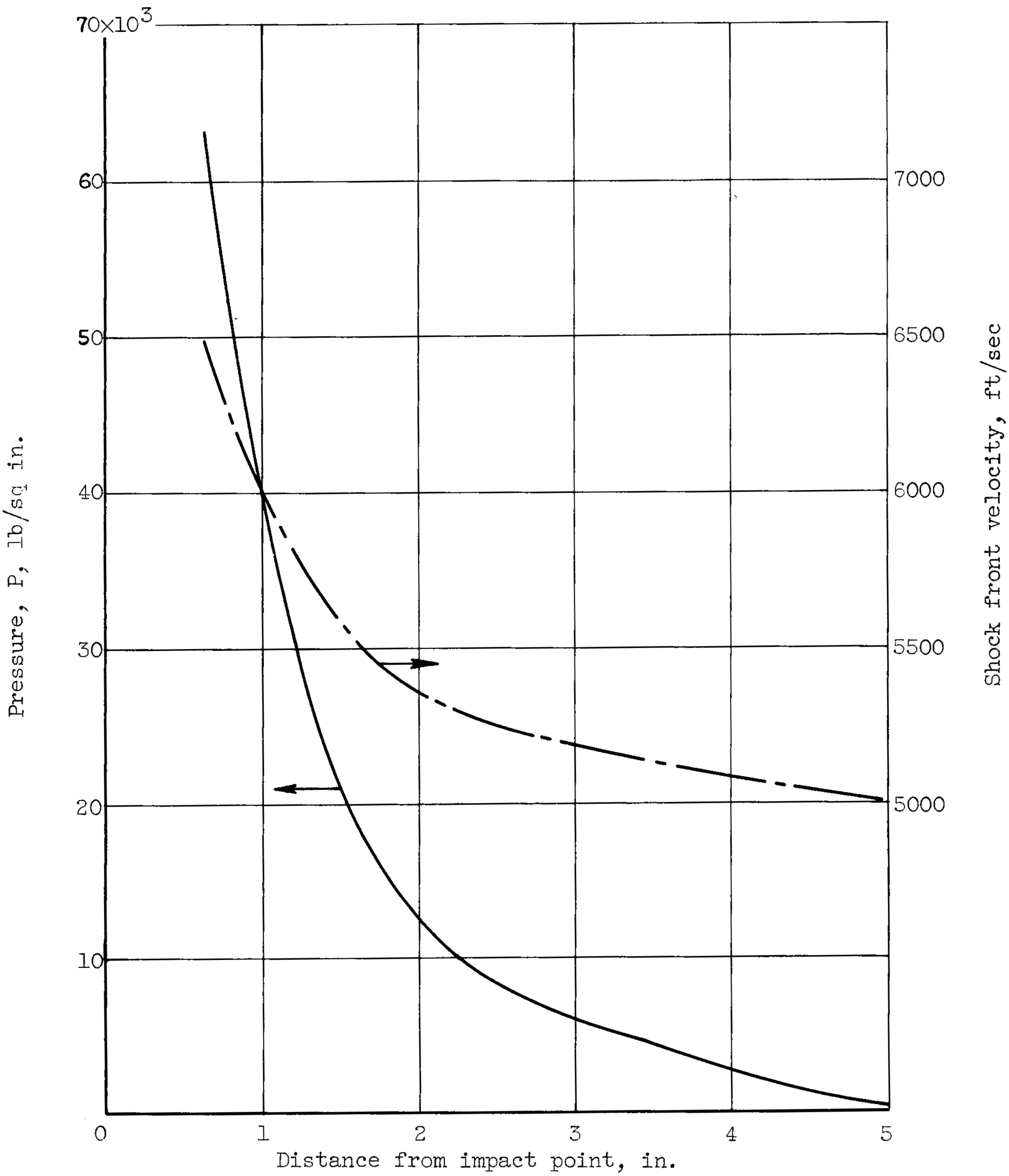

Figure 8. - Pressure and velocity of shock front as generated from impact into water. Impacting particle, 7/32-inch-diameter aluminum sphere; velocity, 6690 feet per second.

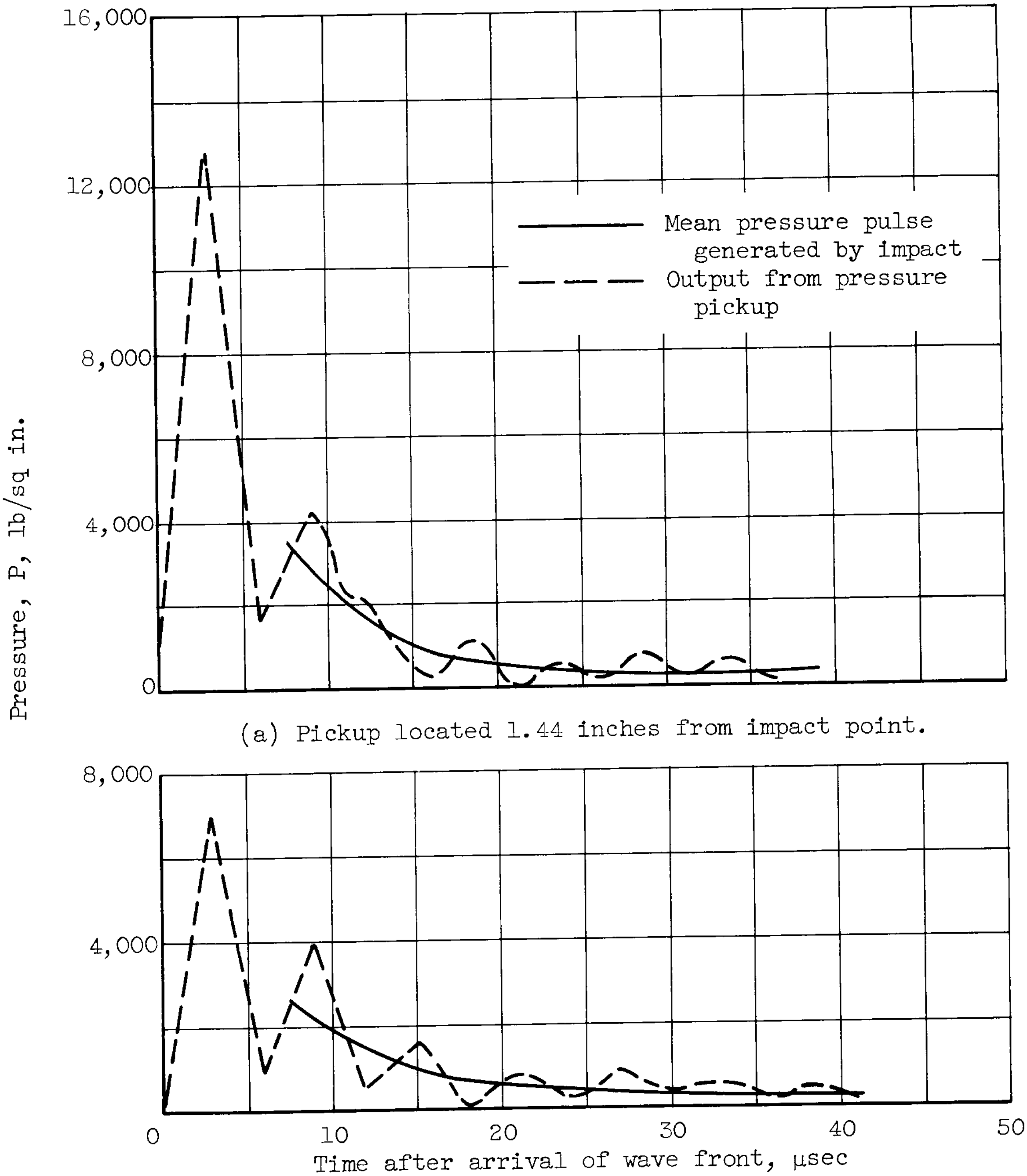

(a) Pickup located 1.44 inches from impact point.

(b) Pickup located 1.87 inches from impact point.

Figure 9. - Pressure pulses generated by impact into water as measured by piezoelectric crystal pickups. Impacting particle, 7/32-inch-diameter aluminum sphere; velocity, 6690 feet per second.

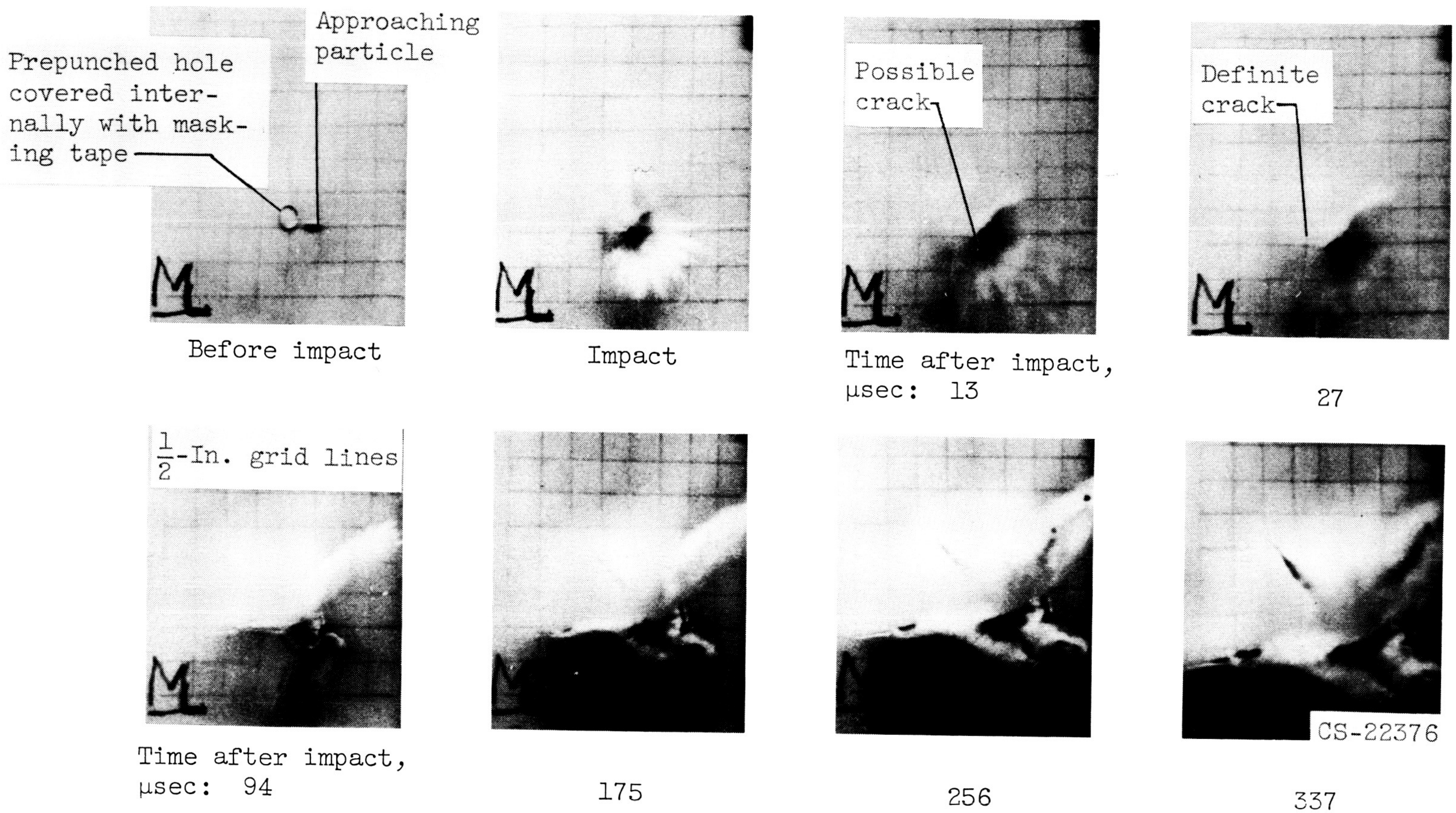

Figure 10. - Effect of high-speed particle impact into water through prepunched hole in 1/32-inch-thick 7075-T6 aluminum sheet. Impacting particle, 7/32-inch aluminum sphere; velocity, approximately 6200 feet per second.

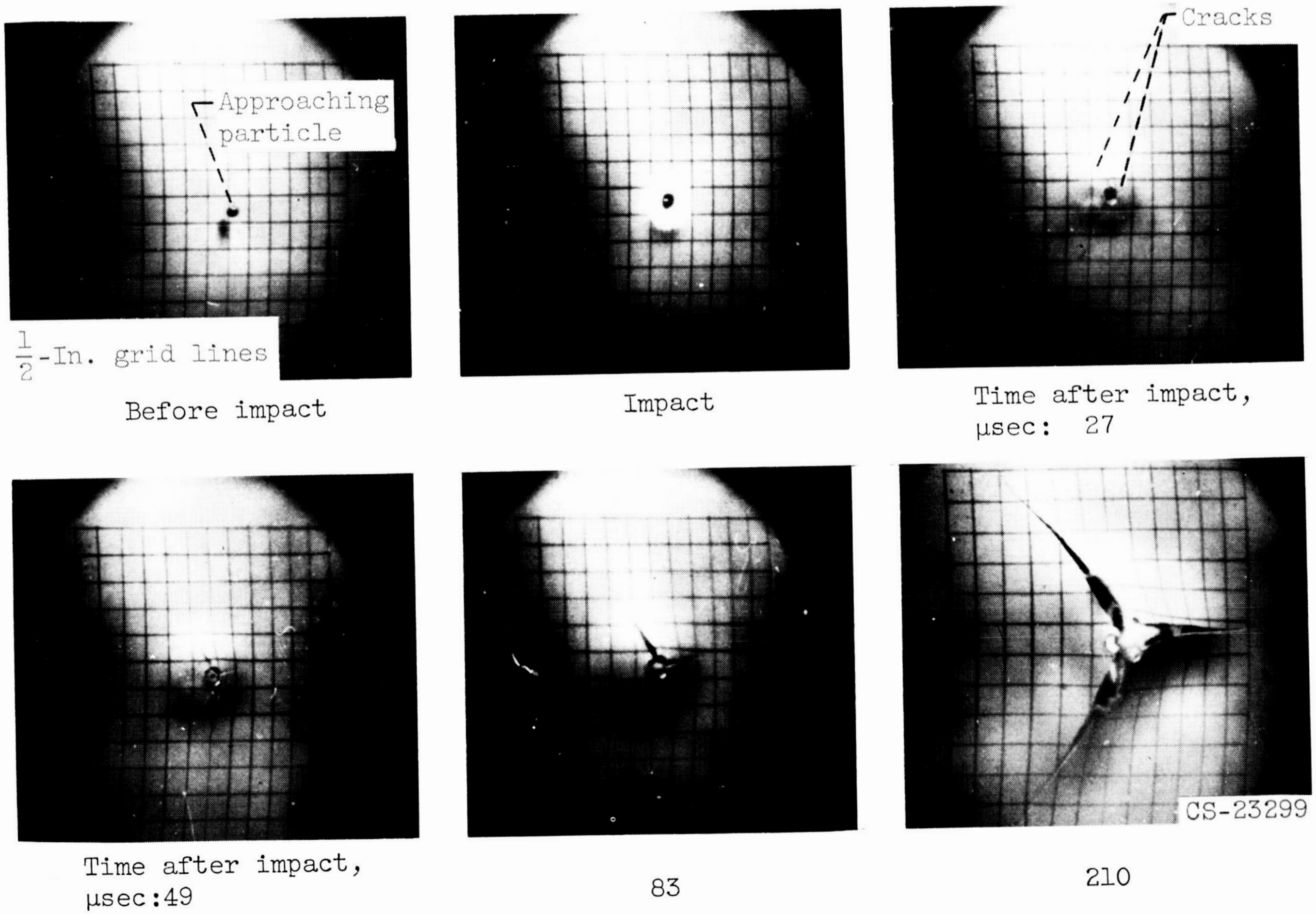

Figure 11. - Effect of high-speed particle impact into stressed specimen of 1/32-inch-thick 7075-T6 aluminum on water-filled tank. Impacting particle, 7/32-inch aluminum sphere; velocity, 5780 feet per second.